Complex Dynamics and Bifurcation in a Two-Ring System With Phase Control

Valerie P. Ponomarenko

Research Institute of Applied Mathematics and Cybernetics,
Nizhni Novgorod, Russia, povp@uic.nnov.ru

Abstract

Modes of dynamic behavior in a coupled system with phase and time-delay control are studied. The system is intended for tracking estimation of a complex signal's parameters. The case is considered when one of the subsystems individually demonstrates simple regular dynamics while the other subsystem exhibits both regular and chaotic dynamical states. The behavior of the examined system is described by nonlinear fore-dimensional set of differential equations with periodical nonlinearity. The bifurcation diagram is determined, the regions with the state of phase synchronization, periodic and chaotic nonsynchronous modes of interacting subsystems are found. Scenarios of development of nonsynchronous modes under variation of the system parameters are established. The possibilities of control over properties and domains of existence of dynamical regimes are ascertained by varying of system's parameters values.

I. Introduction

The study of complex dynamics phenomena and bifurcation transitions in coupled auto-oscillation systems is of interest in several fields of science and engineering. Interacting oscillators with feedback loops that perform automatic phase or frequency control take a significant place in the family of coupled oscillation systems. In this paper, we investigate a system created on the basis of a two-ring synchronizing system (TRSS) integrating coupled subsystems intended for automatic phase control (APC) and automatic time-delay control (ATDC). Different versions of system with such structure are of interest because they represent a circuit implementation of optimal algorithms for tracking estimation of variable parameters (phase angle $\vartheta(t)$ and time delay $T(t)$) of pseudorandom phase-shift keyed radio signals [1,2]. Such complex signals are used actively in the modern wideband communication systems for transmission and processing of information. In addition, application of TRSS creates wide possibilities for generation of various types of chaotic oscillations. Thus, these systems may be promising for devices where information is transmitted via chaotic signals.

Knowledge of the specific features of the nonlinear dynamics for various TRSS versions, mechanisms for excitation and evolution dynamical states and for chaotization, and ways of governing the behavior of the systems is of significant importance during the process of making a justified decision regarding implementation of a particular version of a system's structure in specific applications. The global dynamical behavior of a TRSS is completely determined by the subsystems control loops parameters, parameter of coupling and initial frequency and delay detuning. We study in this paper the dynamical modes and nonlinear phenomena observed from a TRSS's model in the case where the subsystems are coupled by means of connecting the ATDC's output to the APC's input, which is needed to demodulate the received signal, and by control circuits. Owing to the connection through control circuits, the phase mismatch signal generated in the APC loop is sent to the delay control circuit.

II. TRSS model under consideration

Equations describing the dynamics of the considered TRSS can be derived from the equations for estimated values ϑ^* and T^* of parameters $\vartheta(t)$ and $T(t)$, obtained in [2,3]. These equations can be represented for mismatches $\varphi=\vartheta(t)-\vartheta^*(t)$ $\eta=T(t)-T^*(t)$ in the operator form ($p\equiv d/dt$) as follows [4,5]:

$$\varphi = \vartheta - (k_1 / p)K_1(p)R(\eta)sin\varphi,$$
$$\eta = T - T_0 - K_2(p)[k_2 D(\eta) + k_3 R(\eta)sin\varphi], \quad (1)$$

where k_1 and k_2 are the amplification factors of subsystem's control circuits; k_3 is the factor of coupling via control signals; T_0 is the initial delay of the signal generated in an ATDC subsystem; $K_1(p)$ and $K_2(p)$ are the transfer functions of the low-frequency filters (LFFs) in the APC and ATDC control circuits; $R(\eta)$ is the correlation function of the modulating signal, it may be interpreted as coupling nonlinearity introduced into APC subsystem by ATDC subsystem; $sin\varphi$ and $D(\eta)$ are the usual feedback loop nonlinearities – the characteristics of discriminators in APC and ATDC subsystems, respectively. Schematic representation of TRSS corresponding to equations (1) is shown in Fig.1.

The individual behavior of the APC and ATDC subsystems depends substantially on the type of LFFs used in the control circuits. In this paper we will consider the TRSS's dynamics in the case of the second-order filter in the APC subsystem ($K_1(p)=1/(1+(T_1+T_2)p+T_1 T_2 p^2)$) and the first-order filter in ATDC subsystem ($K_2(p)=1/(1+T_3 p)$) where T_1, T_2, and T_3 are the time constant. Note that the considered types of LFFs correspond

to the models for dynamics of parameters ϑ and T used in certain applied problems [1-3]. In this case separate ATDC subsystem demonstrates simple regular modes while isolated APC subsystem exhibits both regular and chaotic modes.
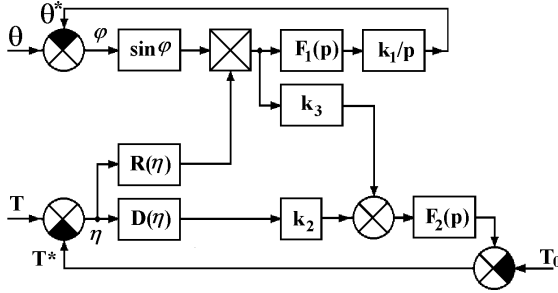

Fig.1. Schematic representation of TRSS

The equations that describe the dynamic of a TRSS with considered LFFs are obtained from the equations (1) and can be written in dimensionless form as [5]

$$\frac{d\varphi}{d\tau} = y,$$

$$\frac{dy}{d\tau} = z,$$

$$\mu \frac{dz}{d\tau} = \gamma - R(x)\sin\varphi - y - \varepsilon_1 z, \qquad (2)$$

$$\varepsilon_2 \frac{dx}{d\tau} = \sigma - x - bD(x) - \alpha R(x)\sin\varphi,$$

where $\tau = k_1 t$, $x = \eta/\tau_0$ (τ_0 is the duration of a signal element in the modulating pseudorandom signal), $\gamma = p\vartheta/k_1$ and $\sigma = (T-T_0)/\tau_0$ are the initial frequency and delay mismatches, respectively, $b = k_2/\tau_0$, $\alpha = k_3 b$, $\varepsilon_1 = (T_1+T_2)k_1$, $\mu = T_1 T_2 k_1^2$, $\varepsilon_2 = T_3 k_1$, $R(x)$ and $D(x)$ are piecewise-linear characteristics having the form [1,2]

$$R(x) = \begin{cases} 1+x, & -1 \le x \le 0, \\ 1-x, & 0 \le x \le 1, \\ 0, & |x| \ge 1, \end{cases} \quad D(x) = \begin{cases} -2-x, & -2 \le x \le -1, \\ x, & -1 \le x \le 1, \\ 2-x, & 1 \le x \le 2, \\ 0, & |x| \ge 2. \end{cases}$$

Dynamical system (2) has cylindrical phase space $U = (\varphi(mod2\pi), y, z, x)$. Investigations of the system (2) are performed using qualitative-numerical methods and computer simulation developed for analysis of nonlinear dynamical systems.

III. Stability of the tracking mode

System (2) with parameters $(\gamma, b, \sigma, \alpha) \in C_0$ where

$$C_0 = \{max(\gamma_3, \gamma_4) < \gamma < min(\gamma_1, \gamma_2)\},$$
$$\gamma_1 = (1+b-\sigma)/(1+b-\alpha), \quad \gamma_2 = (1+b+\sigma)/(1+b+\alpha),$$
$$\gamma_3 = -(1+b+\sigma)/(1+b-\alpha), \quad \gamma_4 = -(1+b-\sigma)/(1+b+\alpha),$$

has two equilibrium states $A_1(\varphi_1, 0, 0, x_1)$ and $A_2(\pi-\varphi_1, 0, 0, x_1)$ located within the range $-1 < x < 1$ of phase space U; coordinates φ_1 and x_1 defined by

$\varphi_1 = arcsin(\gamma/(1-x_1 sgn(\sigma-\alpha\gamma)))$, $x_1 = (\sigma-\alpha\gamma)/(1+b)$. (3)
Equilibrium state A_1 may be either stable or unstable, while equilibrium state A_2 is a saddle-type unstable point. The condition under which equilibrium state A_1 is stable is determined by the roots of the characteristic equation for the eigenvalues of the linearized system near the equilibrium states

$$\lambda^4 + c_1\lambda^3 + c_2\lambda^2 + c_3\lambda + c_4 = 0, \qquad (4)$$

where
$c_1 = \varepsilon_1/\mu + a_1$, $c_2 = (1+\varepsilon_1 a_1)/\mu$, $c_3 = (a_1+a_2)$, $c_4 = (1+b)a_2/(\mu\varepsilon_2)$,
$a_1 = \varepsilon_2^{-1}(1+b-\alpha\gamma sgn(\sigma-\alpha\gamma)/(1-(\sigma-\alpha\gamma)sgn(\sigma-\alpha\gamma)/(1+b)))$,
$\quad a_2 = (1-(\sigma-\alpha\gamma)sgn(\sigma-\alpha\gamma)/(1+b))^2 - \gamma^2)^{1/2}$.

Applying the Routh-Hurwitz criterion to equation (4), we obtain that equilibrium state A_1 is stable for the values of parameters such that the following inequalities hold:

$$c_1, c_2, c_3, c_4 > 0, \quad c_3(c_1c_2-c_3) - c_4c_1^2 > 0. \qquad (5)$$

If condition (5) is satisfied, the studied TRSS has the mode of tracking of an estimated signal's parameters corresponding to equilibrium state A_1. Values φ_1 and x_1 determined by (3) characterize the accuracy with which the parameters of input signal are estimated. The domain C_s where equilibrium state A_1 is stable corresponds to the region, in which the TRSS is holding in the tracking mode.

IV. Nonsynchronous modes and bifurcation

The dynamical modes and bifurcation of the TRSS have been studied by a numerical simulation of the equations (2) [5]. Let us consider received results for case of $\sigma = 1$, $b = 5$, $\alpha = 2$, $\varepsilon_1 = 1$, and $\varepsilon_2 = 2$. Fig.2 shows bifurcation diagram of model (2) on the plane of parameters (μ, γ). Lines γ_2 and γ_4 are the boundaries of domain $C_0 = \{\gamma_4 < \gamma < \gamma_2\}$ in which the equilibrium states A_1 and A_2 exist. Curve γ_s corresponds to the loss of the tracking mode stability. Domain C_s where the tracking mode is stable is located between curves γ_2, γ_4, and γ_s. When, as a result of growing μ, the system crosses the curve γ_s, conditions (5) is violated and system (2) exhibits the Andronov-Hopf bifurcation. The latter is related to a solution of characteristic equation (4) containing a pair of complex-conjugated roots with a positive real part. At the same time, oscillatory type limit cycle O_1 such that phase difference φ varies within a limited range not exceeding 2π appears in phase space U. Cycle O_1 corresponds to a quasi-synchronous mode in the TRSS where periodic oscillations of phase variables are observed around equilibrium state A_1 that has become unstable. Quasi-synchronous mode of the limit cycle O_1 exists for the values of parameters μ and γ belonging to domain D bounded by curve γ_s and the parts of curves γ_{d1}, γ_{d2}, γ_{c1}, and γ_{c2}. Curves γ_{c1} and γ_{c2} in Fig.2 correspond to saddle-node bifurcation of the oscillatory limit cycles. Curves γ_{d1} and γ_{d2} correspond to the loss of these cycles stability resulting from a period-doubling bifurcation which occurs when the system crosses lines γ_{d1} and γ_{d2} with increasing of μ.
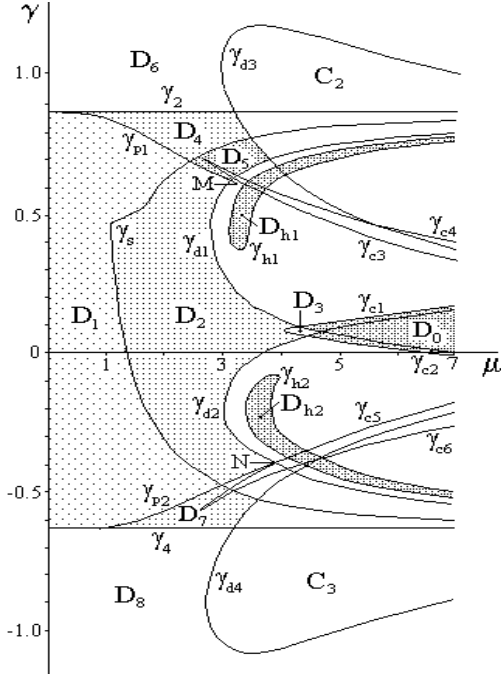
Fig.2. Dynamic mode domains for model (2)

Curves γ_{p1} and γ_{p2} correspond to formation of the stable rotational type separatrix loops Π_φ^+ and Π_φ^-, respectively, of saddle-focus equilibrium state A_2 (the root of characteristic equation (4) for the point A_2 satisfy the following inequalities: $Re\lambda_{1,2}<0$, $Im\lambda_{1,2}\neq0$, $\lambda_3<0$, $\lambda_4>0$). When the curve γ_{p1} (the curve γ_{p2}) is crossed as γ increases (as γ decreases) a stable rotational limit cycle L_1 (limit cycle L_2) with the 2π period in φ appears in the phase space U. These cycles is associated with the asynchronous modes of TRSS such that phase difference φ rotates and variables y,z, and x periodically oscillate about certain mean values. Curves γ_{c3}, γ_{c4}, γ_{c5}, and γ_{c6} correspond to the saddle-node bifurcation of rotational limit cycles. On lines γ_{d3} and γ_{d4} these limit cycles loses its stability as a result of periodic-doubling bifurcation.

For the parameters from domains D_1, D_2, D_3, D_4, D_5, D_6, D_7, and D_8 system (2) demonstrates regular dynamical modes. In domain D_1 restricted by parts of curves γ_2, γ_{p1}, γ_s, γ_{p2}, and γ_4 the system does not have in the phase space U other attractors apart from equilibrium state A_1. Thus, in domain D_1, the tracking mode is realized in TRSS for any initial conditions. In view of this circumstance, we will consider domain D_1 as a locking region of the system.

For parameters from domain D_2 located between the curves γ_s, γ_{p1}, γ_{d1}, γ_{c1}, γ_{c2}, γ_{d2}, and γ_{p2} the quasi-synchronous mode of limit cycle O_1 is realized in the TRSS irrespective to initial conditions.

In domain D_3 restricted by parts of curves γ_{c1}, γ_{d1}, γ_{c2}, and γ_{d2} oscillatory limit cycles O_1 and O_2 are simultaneously exists in the phase space U. Cycle O_2 appears when the system crosses curve γ_{c2} as a result of γ increase or when the system crosses curve γ_{c1} as a result of γ decrease. Depending on initial conditions, either of two quasi-synchronous modes of cycles O_1 and O_2 may

be realized in the TRSS. During a transition that occurs across curve γ_{d1} from domain D_3 limit cycle O_1 undergo period-doubling bifurcation while the mode of limit cycle O_2 is retained in domain restricted by curves γ_{d1}, γ_{c1}, and γ_{d2}. Upon passing out of domain D_3 across curve γ_{d2} a period-doubling bifurcation of limit cycle O_2 is observed in system (2) while the mode of limit cycle O_1 is retained in domain restricted by curves γ_{c2}, γ_{d1}, and γ_{d2}.

For the parameters from domain D_4 located between curves γ_2, γ_{p1}, γ_s, and γ_{d3} the phase trajectories converge to either equilibrium state A_1 or the rotational limit cycle L_1, depending on the initial conditions. Thus, in domain D_4 tracking and asynchronous modes exist in TRSS simultaneously. Tracking mode is realized if the initial conditions fall into basin of attraction of equilibrium state A_1 in the phase space U.

In domain D_5 bounded by curves γ_{p1}, γ_{d1}, γ_s, and γ_{d3} besides the tracking mode and asynchronous mode of limit cycle L_1, the quasi-synchronous mode of limit cycle O_1 were also observed. In addition, upon passing through curve γ_{c3}, as γ is increased or through curve γ_{c4}, as γ is decreased, a stable limit cycle L_3 appears in the phase space U. As a result, for γ and μ values lying between curves γ_{c3} and γ_{c4} nonsynchronous modes of the limit cycles O_1, L_1, and L_3 may be realized in the TRSS. The initial conditions determine which of these modes is realized in domain D_5.

When parameters γ and μ have values falling into the domain D_6 between the γ_2 and γ_{d3} lines, the mode of rotational limit cycle L_1 is realized in the TRSS. At the values of γ and μ belonging to domain D_7 bounded by sections of curves γ_4, γ_{d4}, γ_{p2}, and γ_s, the TRSS has the tracking mode and two concurrent asynchronous modes determined by limit cycles L_2 and L_4. Note that, the cycle L_4 appears in the phase space U upon passing through curve γ_{c5}, as γ is decreased, or through curve γ_{c6}, as γ is increased. Domain D_8 (between sections of curves γ_4 and γ_{d4}) corresponds to asynchronous mode of limit cycle L_2.

For the parameters from domain $D_c=\{C_0\backslash C_1\}\cup C_2\cup C_3$ the TRSS exhibits both regular and chaotic regimes of oscillations (domain $C_1=\cup D_i$, $i=1,2,3,4,5,6,7$, domain C_2 is restricted by parts of curves γ_{d3} and γ_2 ($\gamma>\gamma_2$), domain C_3 is bounded by parts of curves γ_{d4} and γ_4 ($\gamma<\gamma_4$)). Lines γ_{h1} and γ_{h2} marks the boundary of domains D_{h1} and D_{h2}, where the chaotic attractors of oscillatory type formed through a sequence of limit cycle O_1 period-doubling bifurcations exist in the phase space U. Numerical simulation of system (2) shows that, upon passing out of domains D_{h1} and D_{h2}, as μ is increased, the chaotic regime of the TRSS breaks down and the system enters an asynchronous regime determined by rotational or oscillatory-rotational limit cycle.

V. Evolution of nonsynchronous modes

Let us consider qualitative features of complex dynamics of system (2) exhibited at variable parameters μ

and γ with values lying in domain D_c. For that purpose we analyze to one-parameter bifurcation diagram of the point mapping produced by trajectories of system (2).
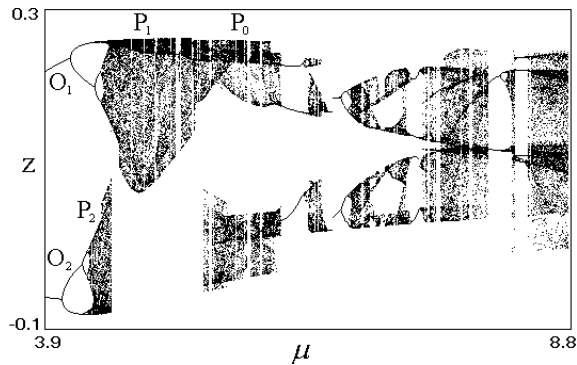

Fig.3. Evolution of the modes of limit cycles O_1 and O_2 observed as μ increases

Fig.3 shows bifurcation diagram$\{\mu, z\}$ calculated at γ=0.085. It characterized evolution of quasi-synchronous modes of limit cycles O_1 and O_2, whose (φ, y) projections of phase portrait are displayed in Fig.4a with variations of parameter μ in domain D_0. The $\{\mu, z\}$ diagram shows that, as μ increases, limit cycles O_1 and O_2 are transformed into chaotic attractors P_2 and P_2 (Figs.4b,c) through period-doubling bifurcations. When μ >4.519, the system rigidly switches from the mode of chaotic attractor P_2 to chaotic oscillations on attractor P_1, the latter persisting until the value 5.388 μ is reached. When μ >5.388, the system passes to chaotic oscillation mode with double-scroll chaotic attractor P_0 containing two loci of chaotic motion with jumps between them (Fig.4d) [6]. Fig.4e shows time realization$\varphi(\tau)$ corresponding to attractor P_0. Note that, the dynamical φ range of this mode exceeds 2π. Trajectories on attractor P_0 scroll around each of the unstable equilibrium states $A_1(\varphi_1, 0, 0, x_1)$ and $A_1*(\varphi_1-2\pi, 0, 0, x_1)$ and also around all three equilibrium states: A_1, A_2, and A_1*.
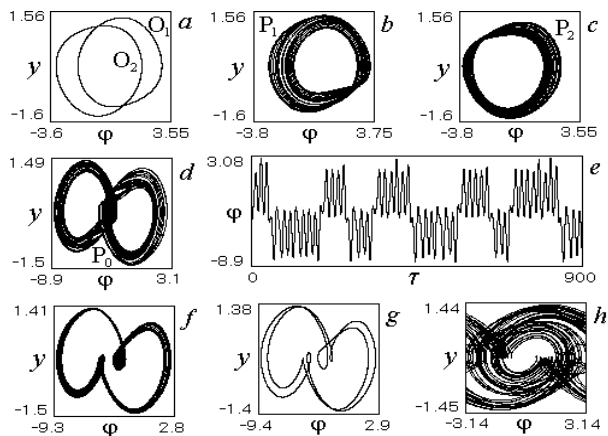

Fig.4. Phase portraits and time realization that correspond to attractors of system (2) for μ=(a) 3.9, (b) 4.7, (c) 4.4, (d,e) 5.5, (f) 6.9, (g) 7.35, (h) 8.55

As μ increases, one observes in Fig.3 alternating chaotic oscillations of attractor P_0 and regular oscilla-

tions of complex limit cycles retaining the character of motions on attractor P_0. Note that, in the attractor structure, the number of trajectories scrolls around each of equilibrium states A_1 and A_1* decreases while scrolls around three equilibrium states A_1, A_2, and A_1* increases. Figs.4f and 4g represent the phase portraits of the mode of chaotic attractor and limit cycle without trajectory scrolls around A_1 and around A_1*. Transitions between regular and chaotic modes are realized both rigidly and via direct and reverse period-doubling bifurcations.

Upon passing the value μ =8.41, the system exhibits the mode of oscillatory-rotational chaotic attractor (Fig.4h). This mode is characterized by irregular alternating oscillations about unstable equilibrium state A_1 and oscillations with rotating phase difference φ. As μ increases, the system exhibits chaotic and regular modes corresponding to oscillatory-rotational attractors of system (2).
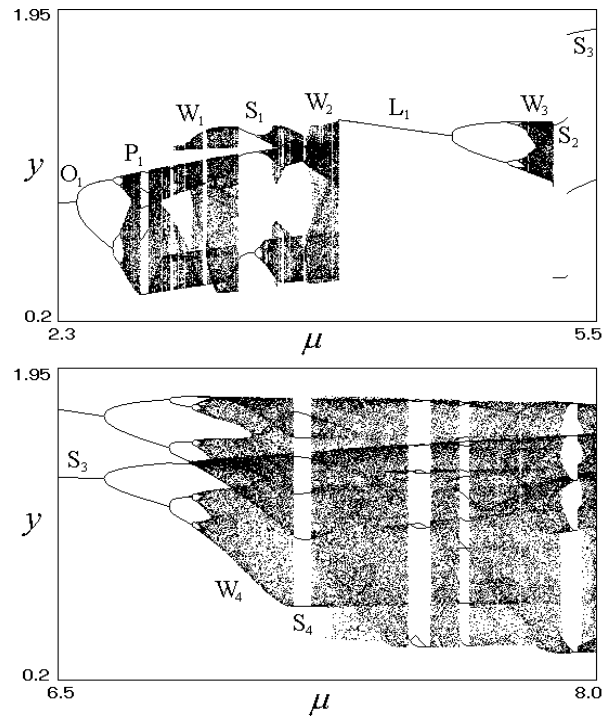

Fig. 5. Evolution of the mode of limit cycle O_1 observed as μ_2 increases

Analyzing bifurcation diagrams calculated for various values of γ, we see that, as γ increases, an interval of μ corresponding to quasi-synchronous modes is decreases. Fig.5 represents bifurcation diagram $\{\mu, y\}$ calculated at γ=0.5. It characterizes the mode of limit cycle O_1 evolution when μ increases from 2.3 to 8.0. It is seen from the diagram that, in the interval 2.3<μ <2.997 alternating periodic and chaotic quasi-synchronous modes are realized in the system. After that, in the interval 2.997<μ<3.969 asynchronous modes corresponding to chaotic attractors and limit cycles of oscillatory-rotational type are observed. Figs.6a,b,c shows the phase portraits corresponding to a chaotic attractor W_1, limit cycle S_1, and chaotic attractor W_2.

When the value of μ falls in interval $3.969<\mu<5.224$, the system exhibits asynchronous modes developing on the base of rotational limit cycle L_1 (Fig.6d). As μ increases, the mode of cycle L_1 are transformed into the mode of chaotic attractor W_3 (Fig.6e) through period-doubling bifurcations. In the interval $5.224<\mu<8.0$, the system again exhibits the mode determined by regular and chaotic attractors of oscillatory-rotational type. Examples of them – limit cycles S_2 and S_3, chaotic attractor W_4 that forms on the base of cycle S_3 via period-doubling bifurcations, and multi turnover limit cycle S_4 are shown in Figs.6f-6i.
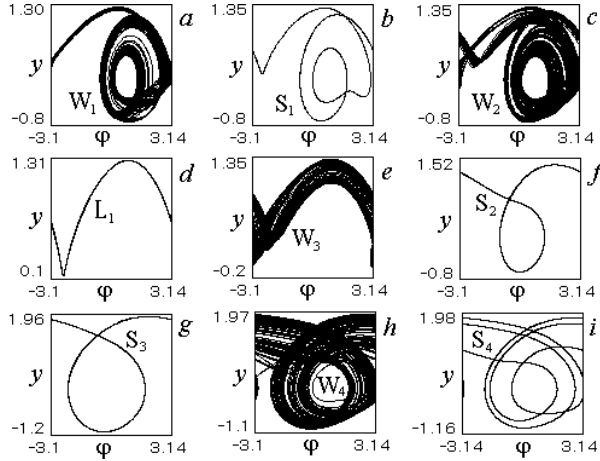

Fig.6. Phase portraits corresponding to attractors of system (2) for $\mu =(a)$ 3.1, (b) 3.4, (c) 3.9, (d) 4.3, (e) 5.2, (f) 5.25, (g) 5.35, (h) 7.25, (i) 7.18

As parameter μ varies in the reverse direction (from 8.0 to 2.3) the bifurcation diagram has another form in the interval $0.387<\mu<5.326$, and hysteresis in the behavior of the system is observed. As μ falls into this interval, the mode of limit cycle S_2 (Fig.6f) converted into the mode of chaotic attractor W_5; after that, the system comes back to the mode of cycle S_2 through bifurcations reverse to period-doubling bifurcations. When $\mu =0.387$ limit cycle S_2 vanishes via a saddle-node bifurcation and, at $\mu <0.387$, the system rigidly switches to the mode of chaotic attractor W_2 (Fig.6c). Hence, in the interval indicated above, the system behavior is bistable. This is due to that fact that oscillatory-rotational and rotational attractors exist in the phase space simultaneously. The initial conditions determine which of these modes is realized in this interval.

Fig.7a shows bifurcation diagram $\{\mu, y\}$ plotted for $\gamma =0.7$; parameter μ ranges from 3.1 to 6.1. The diagram characterizes evolution of quasi-synchronous mode of limit cycle O_1 and asynchronous mode of limit cycle L_1 coexisting at $\mu =3.1$, as μ increases. It is seen that, in the interval $3.1<\mu<4.018$ cycles O_1 and L_1 are transformed into chaotic attractors P_1 (Fig.4b) and W_3 (Fig.6e), respectively, through period-doubling bifurcations. Upon reaching the value $\mu =4.018$, attractor P_1 is destroyed and the system rigidly switches to chaotic oscillations on attractor W_3. When $\mu >4.055$, attractor W_3 is transformed into oscillatory-rotational chaotic

attractor W_6. After that, as μ increases, alternation of the mode of the attractor W_6 and periodic modes of complex oscillatory-rotational limit cycles takes place; in the majority of the interval $4.055<\mu<6.1$, chaotic modes are realized in the system. For that chaotic modes are characterized by irregular alternation of oscillatory, oscillatory-rotational, and rotational motions. Fig.7b displays time waveform $y(\tau)$ corresponding to such a chaotic mode.
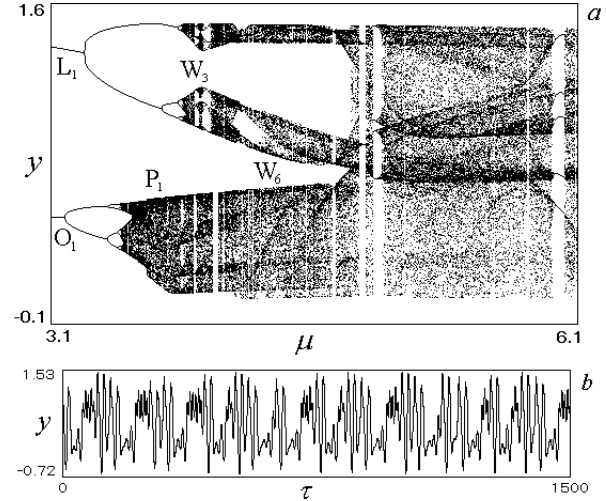

Fig. 7. Evolution of the modes of limit cycles L_1 and O_1, observed as μ increases (a), and time realizations $y(\tau)$ corresponding to the chaotic mode for $\mu =6.35$ (b)

The results represented above show different character of nonsynchronous modes corresponding to the same parameter values and gives possibilities for control of the TRSS behavior modes by change of initial conditions.

Let us discuss nonsynchronous modes of TRSS formed when inertia parameter ε_1 and coupling parameter α varies. In Fig.8 bifurcation diagram $\{\varepsilon_1, y\}$ plotted for the values of $\gamma=0.085$, and $\mu =5.5$ is shown. The mode of oscillatory-rotational chaotic attractor W_7 is the system's starting state for $\varepsilon_1=0.52$. As ε_1 increases, at first, the mode of attractor W_7 is transformed to the quasi-synchronous mode of double-scroll chaotic attractor P_0. When $\varepsilon_1 >0.627$, attractor P_0 is rigidly replaced by limit cycle O_1. In the interval $0.704<\varepsilon_1 <1.029$ the system again exhibits regular and chaotic attractors with transitions between equilibrium states A_1^* and A_1. When value of ε_1 falls in interval $1.029<\varepsilon_1 <1.37$, chaotic and periodic modes of oscillations about equilibrium state A_1 are observed in the system. After that, dechaotization of chaotic quasi-synchronous mode through bifurcations reverse to period-doubling bifurcations develops, and the system passes to quasi-synchronous mode of limit cycle O_1. Further increasing of ε_1 value results in soft transformation of the mode of limit cycle O_1 to the tracking mode of the TRSS.

Fig.9 shows bifurcation diagram $\{\alpha, y\}$ corresponding to $\gamma=0.7$, $\varepsilon_1=0.7$, and $\mu =5.5$. As the initial state of system (2) for $\alpha =0.1$, we choose the mode of oscillatory-rotational chaotic attractor. The bifurcation dia-

gram in Fig.9 characterizes the motions formed in the transformation process of this chaotic mode to the mode of limit cycle O_1. It is seen that, regular and chaotic modes of oscillatory-rotational type are realized in the majority of the studied α range. In the interval $2.919 < \alpha < 3.746$ quasi-synchronous modes are observed; for that, the mode of limit cycle O_1 is realized in the interval $3.162 < \alpha < 3.746$. When α crosses the threshold $\alpha = 3.746$, the system passes to the tracking mode. Then, as α increases, this mode rigidly switches to asynchronous mode.
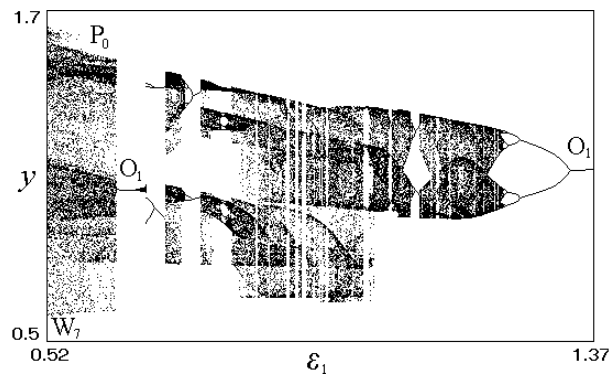

Fig.8. Dynamics of the behavior of system (2)
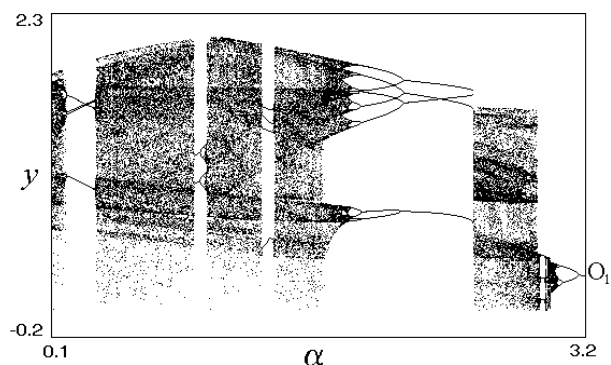when ε_1 is varied

Fig.9. Dynamics of the behavior of system (2)
when α is varied

The results represented in Figs.8 and 9 indicate the opportunity to carry the TRSS from nonsynchronous modes to the tracking mode with the help of suitable selection of parameters ε_1 and α values.

It follows from the results presented above that parameters μ and ε_1 characterizing degree of influence of second-order filter in APC subsystem, parameter of coupling α and initial frequency mismatch γ affect significantly dynamical properties of the system. Specifically, if we choose the system parameters corresponding to oscillatory or oscillatory-rotational chaotic attractors then, such TRSS may be regarded as a generator of chaotic oscillations.

V. Conclusion

In this paper, the modes of behavior peculiar to a two-ring system of coupled APC and ATDC subsystems are investigated within a framework of dynamic model with four degrees of freedom. Using this model, we revealed characteristic features of the collective behavior of the subsystems when individual dynamics of APC subsystem is characterized by the existence of both synchronous and asynchronous modes, that may be as regular as chaotic, and ATDC subsystem has simple regular dynamics. Investigation of model (2) enables one to classify dynamical modes that are characteristic of the TRSS under study: the tracking mode, periodic quasi-synchronous modes that arise due to Andronov-Hopf and saddle-node bifurcations; regular asynchronous modes that appears due to bifurcations of separatrix loop and saddle-node limit cycles of rotational and oscillatory-rotational type; chaotic quasi-synchronous and asynchronous modes that are formed through period-doubling bifurcations and also in a rigid manner as a result of saddle-node bifurcations of limit cycles.

The obtained results show that such system exhibits interesting dynamic phenomena: the loss of stability of the synchronous mode, existence of regular asynchronous modes determined by limit cycles of different complexity, appearance quasi-synchronous mode of double-scroll chaotic attractor with phase variables irregular switching, different scenarios of dynamical modes evolution when parameters of the system are varied. It is remarkable that complex dynamical modes and transitions to chaotic behavior are observed in the system at relatively low values of the inertiality parameters of the control circuits. The dynamical modes and nonlinear phenomena in model (2) are of fundamental importance for understanding the behavior of the TRSS considered when the tracking mode (synchronous state) is cut off as a result of the system parameters or initial conditions perturbation. Diversity of dynamical modes and bifurcation transitions discovered in the considered version of TRSS structure create broad possibilities towards formation of various signals with the spectra of different complexity.

References

1. G.I. Tuzov, Statistical Theory of Complex-Signal Reception (Sovetskoe Radio, Moscow, 1977) [in Russian].
2. G.I. Tuzov, V.A. Sivov, V.I. Prytkov, et al., Noise Immunity of Radio Systems with Complex Signals, Ed. by G.I. Tuzov (Radio i Svyaz', Moscow, 1985) [in Russian].
3. G.I. Tuzov and V.I. Prytkov, Phase-Locking System, Ed. by V.V. Shakhil'dyan and L.N. Belyustina (Radio I Svyaz', Moscow, 1982) [in Russian], Chap. 7, p. 104.
4. V.P. Ponomarenko, Izvestiya Ross. Akad. Nauk, Teor. Sist. Upr., No. 1, p. 115 (1999).
5. V.P. Ponomarenko, Izvestiya VUZ. Prikladnaya nelineinaya dinamica (Applied Nonlinear Dynamics), Vol. 11 No. 1. p. 47 (2003).
6. V.P. Ponomarenko and E.A. Tikhonov, Radiotekh. Elektron. (Moscow), Vol. 49, No. 2, p.205 (2004).